
Molecular Crystals and Liquid Crystals Science and Technology. Section A. Molecular Crystals and Liquid Crystals

Publication details, including instructions for authors and subscription information:
http://www.tandfonline.com/loi/gmcl19

# Small Angle Light Scattering from Axial Nematic Droplets

Jiandong Ding [a] & Yuliang Yang [a]

[a] Institute of Material Science, Fudan University, Shanghai, 200433, P. R. China

Version of record first published: 04 Oct 2006.

To cite this article: Jiandong Ding & Yuliang Yang (1994): Small Angle Light Scattering from Axial Nematic Droplets, Molecular Crystals and Liquid Crystals Science and Technology. Section A. Molecular Crystals and Liquid Crystals, 238:1, 47-60

To link to this article: http://dx.doi.org/10.1080/10587259408046915

*Mol. Cryst. Liq. Cryst.*, 1994, Vol. 238, pp. 47–60
Reprints available directly from the publisher
Photocopying permitted by license only

Printed in the United States of America



# Small Angle Light Scattering from Axial Nematic Droplets

JIANDONG DING and YULIANG YANG†

*Institute of Material Science, Fudan University, Shanghai 200433, P. R. China*

*(Received January 18, 1993; in final form March 3, 1993)*

Small angle light scattering (SALS) from the three dimensional anisotropic spherical nematic droplets with an axial director configuration is investigated theoretically in this paper. The authors have performed an analytical interpretation for the light scattering from a single axial nematic droplet, considering an arbitrary orientation of the principal symmetry axis of the droplet. Series of scattering patterns for the axial nematic droplets are presented graphically and compared with each other as well as with those for the ideal spherulites or the radial nematic droplets. The dependence of $V_v$ scattering on relative polarizabilities between liquid crystals and isotropic matrices is elucidated. The average size of the axial nematic droplets can readily be determined according to the formulae obtained. Hence it is very prospective to apply SALS to distinguish the director configurations of nematic droplets and to make further extensive studies on composite materials containing anisotropic particles such as polymer dispersed liquid crystal (PDLC).

*Keywords: small angle light scattering, nematic droplets, axial director configuration*

## 1. INTRODUCTION

Small angle light scattering (SALS) is an important method to probe supermolecular structures. Especially, the light scattering from small, optically anisotropic particles is a classic physical problem, and few corresponding analytical solutions have been obtained over the last hundred years.[1-3] Stein *et al.*[4] made an analytical interpretation for the light scattering from polymer spherulites in 1960, which laid a foundation to explore the structures of spherulites by SALS and resulted in great success.[5,6] In this paper, the authors derive the analytical formulae of SALS from an axial nematic droplet, a kind of more complicated three dimensional anisotropic entities, in order to distinguish and measure the nematic droplets by SALS.

Nematic droplets are complex liquid crystalline systems, which can be self-organized in various ways.[7] Recently, polymer dispersed liquid crystal (PDLC) prepared by dispersing nematic droplets into a polymer matrix has attracted both theoretical and experimental physicists.[7-12] It is very prospective for large-area

†To whom the correspondence should be addressed.

displays. Due to the studies on PDLC, nematic droplets have reemerged as a topic of interest.

In the physics of liquid crystals, the concept of director is introduced to represent the principal orientation of a cluster of nematic molecules, and the spatial arrangement of directors is usually called the director configuration.[13] The director configuration in a nematic droplet results from the surface interaction and the interplay of elastic constants.[14] According to Reference 7, there are three typical director configurations of nematic droplets called radial, bipolar and axial, as shown in Figure 1. Since the field response of a nematic droplet is effected by its director configuration, it is very important both in theory and in application to distinguish the director configurations of nematic droplets. Polarized optical microscopy (POM) has been proven a convenient means to differentiate director configurations with the advantage that every single droplet can be displayed under a polarizing microscope.[9,12] The droplet observed by POM usually has the diameter of 5–100 μm, and submicron nematic droplets cannot be seen clearly. Golemme *et al.*[15] has developed $^2$H-NMR to monitor the director configurations of nematic droplets. That technique may be very useful in the case of submicron nematic droplets, but it requires the use of deuterated liquid crystal samples. The nematic droplets on PDLC films have a typical radius of about 0.5–10 μm, which are suitable for SALS studies.

SALS from an optically soft sphere has been treated by some approximate approaches: Rayleigh-Gans approximation for small, submicron nematic droplets[16]; the anomalous diffraction approximation for large droplets[17]; and the geometrical-optics approximation for very large objects.[18] Based on these, light extinction of a PDLC film can be evaluated.[19] In this paper, exact solutions for SALS from axial nematic droplets are obtained, which are not limited only to submicron or micron droplets and have no restriction to the orientation of the droplet axis at all.

Optically, SALS from a radial nematic droplet is the same as that from a polymer spherulite, which has been studied extensively.[4,5] Bipolar and axial nematic droplets are more complex entities, mainly because the symmetries of their optical constants do not coincide with those of droplet shapes. The theoretical and experimental

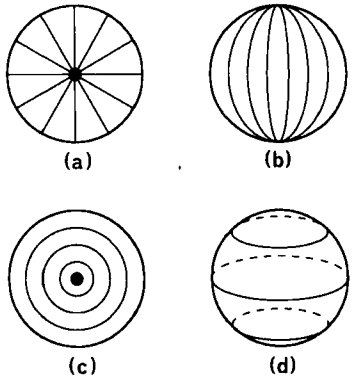


FIGURE 1 Three typical director configurations of nematic droplets: a) radial; b) bipolar; c) and d) axial.

studies on bipolar droplets will be reported by us in another paper.[20] It is also very meaningful to investigate axial nematic droplets. However, there has been, to our knowledge, no light scattering experiment of axial nematic droplets reported in the literature since Drzaic made the first observation of the axial director configuration in 1988.[7] An important reason is that no pertinent theoretical scattering patterns has been presented. Explored in this paper are just the theoretical studies on axial nematic droplets. An analytical interpretation for SALS from an axial nematic droplet immersed in an isotropic matrix is carried out, and series of theoretical scattering patterns are given graphically. In our opinion, this may turn out to be a useful reference for later analysis of relevent scattering patterns observed experimentally. As a conclusion, SALS can serve to distinguish director configurations of nematic droplets and to make further extensive studies on self-organized structures of nematic droplets in composite materials such as PDLC.



## 2. THEORY OF SALS FROM AN AXIAL NEMATIC DROPLET

According to Rayleigh-Debye scattering theory, a model method is used to deal with the SALS from an axial nematic droplet immersed in an isotropic matrix. A single droplet is treated at first. The object is assumed to be optically soft, which is justified.[16-18] The well-known notations used by Stein *et al.*[1-6] are employed. The scattered amplitude can be expressed in terms of the conventional integral[1-4]:

$$E_s = K \int (\mathbf{M} \cdot \mathbf{O}) e^{-ik\mathbf{r}\cdot\mathbf{s}} \, d\Omega \tag{1}$$

where $\mathbf{M}$ is the dipole moment induced by the incident electric field in the volume element at the vector distance $\mathbf{r}$; $\mathbf{O}$ is a unit vector parallel with the direction of the analyzer; $k$ is the wave number $2\pi/\lambda_m$, where $\lambda_m$ is the wave length within matrix; the propagation vector $\mathbf{s}$ is defined as $\mathbf{s} = \mathbf{s}_0 - \mathbf{s}'$, where $\mathbf{s}_0$ and $\mathbf{s}'$ are the unit vectors along the incident and scattered beams, respectively.

The scattering geometry for the axial nematic droplet is defined as in Figure 2, where the $(x, y, z)$ coordinate system is the droplet axis frame with the $z$-axis located at the principal symmetry axis of the droplet, while the $(X, Y, Z)$ coordinate system is the lab frame which is determined by the directions of the light incidence and the light polarization. $\Theta$ and $\Phi$ are the nutation angle and the precession angle respectively. Since the axial droplet has a cylindrical symmetry, $y$-axis can be confined in the $XOY$ plane. The rotation angle is therefore fixed at zero.

The nematic directors in the axial droplet are arranged concentrically around a central core running through the center of the droplet, and they are aligned tangentially on the droplet surface. For convenience, we assume reasonably that the nematic directors are arranged along series of ellipsoids, layer by layer. The ellipsoid shown in Figure 2 has a long principal axis with length of $R$ and two short principal axes with length of $R'$. The ratio of the short and long axes is defined as $f$ with $f = R'/R$, where $f \in (0, 1)$. Obviously, the vector distance $\mathbf{r}$ can be written as

$$\mathbf{r} = R(f \sin\alpha \cos\varphi \mathbf{i} + f \sin\alpha \sin\varphi \mathbf{j} + \cos\alpha \mathbf{k}) \tag{2}$$

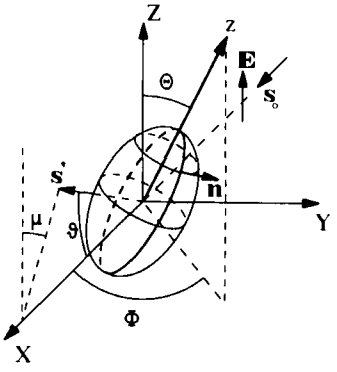


FIGURE 2 The coordinate systems for describing SALS from an axial nematic droplet. $(X, Y, Z)$ is the lab frame while $(x, y, z)$ is the droplet axis frame with $z$-axis located at the principal symmetry axis of the droplet, the orientation of which is described by $\Theta$ and $\Phi$. The $\mathbf{s}_0$, $\mathbf{E}$ and $\mathbf{s}'$ are unit vectors along the directions of incidence, polarization and scattering, respectively. The scattered beam is described by $\vartheta$ and $\mu$. $\mathbf{n}$ refers to the local optical director in the axial nematic droplet.

where $\mathbf{i}$, $\mathbf{j}$ and $\mathbf{k}$ are the basic vectors of the droplet axis frame; $\alpha$ and $\varphi$ are two angles in the ordinary spherical coordinate system with respect to this frame. By Jacobian transformation from Cartesian coordinates, we have

$$d\Omega = \mathbf{R}^3 f \sin^3\alpha \, df \, d\alpha \, d\varphi \tag{3}$$

The propagation vector follows that

$$\mathbf{s} = 2 \sin\frac{\vartheta}{2}\left(\sin\frac{\vartheta}{2}\mathbf{I} - \cos\frac{\vartheta}{2}\sin\mu\mathbf{J} - \cos\frac{\vartheta}{2}\cos\mu\mathbf{K}\right) \tag{4}$$

where $\mathbf{I}$, $\mathbf{J}$ and $\mathbf{K}$ are the basic vectors of the lab frame; $\vartheta$ and $\mu$ are the scattering angle and the azimuthal angle respectively, as defined as in Figure 2. After transforming $\mathbf{s}$ into the droplet axis frame, we get

$$\mathbf{kr}\cdot\mathbf{s} = U(s_1 f \sin\alpha\cos\varphi + s_2 f \sin\alpha\sin\varphi + s_3\cos\alpha) \tag{5}$$

where

$$U = 2kR\sin\frac{\vartheta}{2} = \frac{4\pi R}{\lambda_m}\sin\frac{\vartheta}{2} \tag{6}$$

$$s_1 = \sin\frac{\vartheta}{2}\cos\Theta\cos\Phi - \cos\frac{\vartheta}{2}\sin\mu\cos\Theta\sin\Phi + \cos\frac{\vartheta}{2}\cos\mu\sin\Theta \tag{7.1}$$

$$s_2 = -\sin\frac{\vartheta}{2}\sin\Phi - \cos\frac{\vartheta}{2}\sin\mu\cos\Phi \tag{7.2}$$

$$s_3 = \sin\frac{\vartheta}{2}\sin H\cos\Phi - \cos\frac{\vartheta}{2}\sin\mu\sin\Theta\sin\Phi - \cos\frac{\vartheta}{2}\cos\mu\cos\Theta \tag{7.3}$$

Under the condition of the uniaxial symmetry of the polarizabilities, the vector **M** can be separated into two parts, parallel and perpendicular to the director, then we have

$$\mathbf{M} = \mathbf{M}_{\parallel} + \mathbf{M}_{\perp} \tag{8}$$

$$\mathbf{M}_{\parallel} = (\alpha_{\parallel} - \alpha_s)(\mathbf{E}\cdot\mathbf{n})\mathbf{n} \tag{9}$$

$$\mathbf{M}_{\perp} = (\alpha_{\perp} - \alpha_s)[\mathbf{E} - (\mathbf{E}\cdot\mathbf{n})\mathbf{n}] \tag{10}$$

where **n** is the director, $\alpha_{\parallel}$ and $\alpha_{\perp}$ are polarizabilities parallel and perpendicular to the director respectively, and $\alpha_s$ is the polarizability of the isotropic matrix, **E** is the vector of the polarized incident electric field. The axial director can be expressed as

$$\mathbf{n} = \frac{\partial\mathbf{r}/\partial\varphi}{|\partial\mathbf{r}/\partial\varphi|} = -\sin\varphi\mathbf{i} + \cos\varphi\mathbf{j} \tag{11}$$

In this paper, *Hv* and *Vv* scatterings are investigated, which refer to the scatterings with the analyzer perpendicular and parallel to the polarization of the incident light respectively. Therefore, **E** and **O** may follow that

$$\mathbf{E} = E_0\mathbf{K} = E_0(-\sin\Theta\mathbf{i} + \cos\Theta\mathbf{k}) \tag{12}$$

$$\mathbf{O}(H_v) = \mathbf{J} = \sin\Phi\cos\Theta\mathbf{i} + \cos\Phi\mathbf{j} + \sin\Phi\sin\Theta\mathbf{k} \tag{13}$$

$$\mathbf{O}(V_v) = \mathbf{K} = -\sin\Theta\mathbf{i} + \cos\Theta\mathbf{k} \tag{14}$$

Substituting Equations (11)–(14) into Equations (9)–(10), we have

$$\mathbf{M}_{\parallel}\cdot\mathbf{O}(Hv) = \alpha_{\parallel}E_0\sin\Theta(-\cos\Theta\sin\Phi\sin^2\varphi + \cos\Phi\sin\varphi\cos\varphi) \tag{15}$$

$$\mathbf{M}_{\perp}\cdot\mathbf{O}(Hv) = -\frac{\alpha_{\perp}}{\alpha_{\parallel}}\mathbf{M}_{\parallel}\cdot\mathbf{O}(Hv) \tag{16}$$

$$\mathbf{M}_{\parallel}\cdot\mathbf{O}(Vv) = \alpha_{\parallel}E_0\sin^2\Theta\sin^2\varphi \tag{17}$$

$$\mathbf{M}_{\perp}\cdot\mathbf{O}(Vv) = \alpha_{\perp}E_0 - \frac{\alpha_{\perp}}{\alpha_{\parallel}}\mathbf{M}_{\parallel}\cdot\mathbf{O}(Vv) \tag{18}$$

Again, substituting Equations (3) and (15)–(18) into Equation (1), we can obtain the integral expressions for $Hv$ and $Vv$ scattered amplitudes:

$$E_{H_v} = KE_0R^3\alpha_{12}\sin\Theta\int_0^{2\pi}\int_0^{\pi}\int_0^1 f\sin^3\alpha(-\cos\Theta\sin\Phi\sin^2\varphi + \cos\Phi\sin\varphi\cos\varphi)e^{-ik\mathbf{r}\cdot\mathbf{s}}\,df\,d\alpha\,d\varphi \tag{19}$$

$$E_{V_v} = KE_0R^3\int_0^{2\pi}\int_0^{\pi}\int_0^1 f\sin^3\alpha(\alpha_{20} + \alpha_{12}\sin^2\Theta\sin^2\varphi)e^{-ik\mathbf{r}\cdot\mathbf{s}}\,df\,d\alpha\,d\varphi \tag{20}$$

where

$$\alpha_{12} = \alpha_{\parallel} - \alpha_{\perp} \tag{21}$$

$$\alpha_{20} = \alpha_{\perp} - \alpha_s \tag{22}$$

From the definition

$$I_{mn} = \int_0^{2\pi}\int_0^{\pi}\int_0^1 f\sin^3\alpha(\sin\varphi)^m(\cos\varphi)^n e^{-ik\mathbf{r}\cdot\mathbf{s}}\,df\,d\alpha\,d\varphi \tag{23}$$

$E_{H_v}$ and $E_{V_v}$ can be written as

$$E_{H_v} = KE_0R^3\alpha_{12}\sin\Theta(-\cos\Theta\sin\Phi I_{20} + \cos\Phi I_{11}) \tag{24}$$

$$E_{V_v} = KE_0R^3(\alpha_{20}I_{00} + \alpha_{12}\sin^2\Theta I_{20}) \tag{25}$$

Since a symmetry point at the center of the axial nematic droplet exists, the term $\exp(-ik\mathbf{r}\cdot\mathbf{s})$ in Equation (23) can be simplified to $\cos(k\mathbf{r}\cdot\mathbf{s})$. Expanding $\cos(k\boldsymbol{\gamma}\cdot\mathbf{s})$ into a series and integrating term by term, we obtain

$$I_{00} = \frac{4\pi}{U^3}(\sin U - U\cos U) \tag{26}$$

$$I_{20} = \frac{4\pi}{(1-s_3^2)^2U^3}\left\{s_2^2(1-s_3^2)(\sin U - U\cos U) + \frac{s_2^2 - s_1^2}{s_3}[s_3\sin U - \sin(Us_3)]\right\} \tag{27}$$

$$I_{11} = \frac{4\pi}{U^3}\frac{s_1s_2}{(1-s_3^2)^2}\left\{(1-s_3^2)(\sin U - U\cos U) + \frac{2}{s_3}[s_3\sin U - \sin(Us_3)]\right\} \tag{28}$$

Substituting Equations (26)–(28) into Equations (24) and (25), the scattered amplitudes from a single axial nematic droplet with an arbitrary orientation of the droplet axis can be written analytically as follows:

$$E_{H_v} = KE_0V\frac{3}{U^3}\cdot\frac{\alpha_{12}\sin\Theta}{(1-s_3^2)^2}\cdot\{H_1(\sin U - U\cos U) + H_2[s_3\sin U - \sin(Us_3)]\} \quad (29)$$

where

$$H_1 = s_2(1-s_3^2)\left(\sin\frac{\vartheta}{2}\cos\Theta + \cos\frac{\vartheta}{2}\cos\mu\sin\Theta\cos\Phi\right) \quad (30.1)$$

$$H_2 = \frac{1}{s_3}[\cos\Theta\sin\Phi(s_1^2 - s_2^2) + 2s_1s_2\cos\Phi] \quad (30.2)$$

and

$$E_{V_v} = KE_0V\frac{3}{U^3}\left\{\alpha_{20}(\sin U - U\cos U) + \frac{\alpha_{12}\sin^2\Theta}{(1-s_3^2)^2}\cdot\left[s_2^2(1-s_3^2)(\sin U - U\cos U) + \frac{s_2^2 - s_1^2}{s_3}(s_3\sin U - \sin(Us_3))\right]\right\} \quad (31)$$

When $\alpha_{12}$ equals zero, namely, $\alpha_{\parallel} = \alpha_{\perp} = \alpha$, the formulae are reasonably reduced to those describing SALS from an isotropic sphere:

$$E_{H_v} = 0 \quad (32)$$

$$E_{V_v} = KE_0V\frac{3}{U^3}(\alpha - \alpha_s)(\sin U - U\cos U) \quad (33)$$

It is interesting to note that when $\Theta$ equals zero, SALS from an axial nematic droplet is also the same as that from an isotropic sphere. This result can be readily understood after considering the specific orientation of the droplet axis with respect to the polarizers in this case, which verifies our derivation further.

## 3. SERIES OF SCATTERING PATTERNS

### 3.1. Scattering Patterns for Seven Typical Orientations of an Axial Nematic Droplet

Different from a radial one, the axial nematic droplet has a symmetry axis, therefore the orientation of the droplet axis must be taken into consideration. Special at-

tention is paid to seven typical orientations by us. From the formulae given above, the analytical expression for the scattered amplitude from an axial nematic droplet with any specific orientation can be written down easily. A series of scattering patterns have been calculated. Series of $H_v$ and $V_v$ scattering patterns for different orientations are shown in Figures 3 and 4. For each pattern, corresponding orientational angles, namely, $\Theta$ and $\Phi$, are marked below.

$V_v$ scattering is sensitive to the relative polarizabilities between anisotropic objects and their isotropic matrices. Typical relative polarizabilities are considered with four groups of proportions of $\alpha_{12}$ and $\alpha_{20}$: (0, 1), (1, 0), (1, 1) and (1, $-1$). The case of (0, 1) refers to an isotropic sphere, therefore corresponding scattering patterns are not shown in Figure 4. $V_v$ scattering for any $\alpha_{\parallel}$, $\alpha_{\perp}$ and $\alpha_s$, in our opinion, results from the sum of two kinds of scatterings in the amplitude way: one is the isotropic type in the case of (0, 1), the other is the anisotropic type in the case of (1, 0), which is contributed only by the anisotropic contrast factor $\alpha_{12}$. This can be seen both from Equation (31) and from scattering patterns in Figure 4. Hence, it is the proportion of $\alpha_{12}$ and $\alpha_{20}$ that determines the final $V_v$ scattering pattern for a nematic droplet with a definite director configuration and a definite

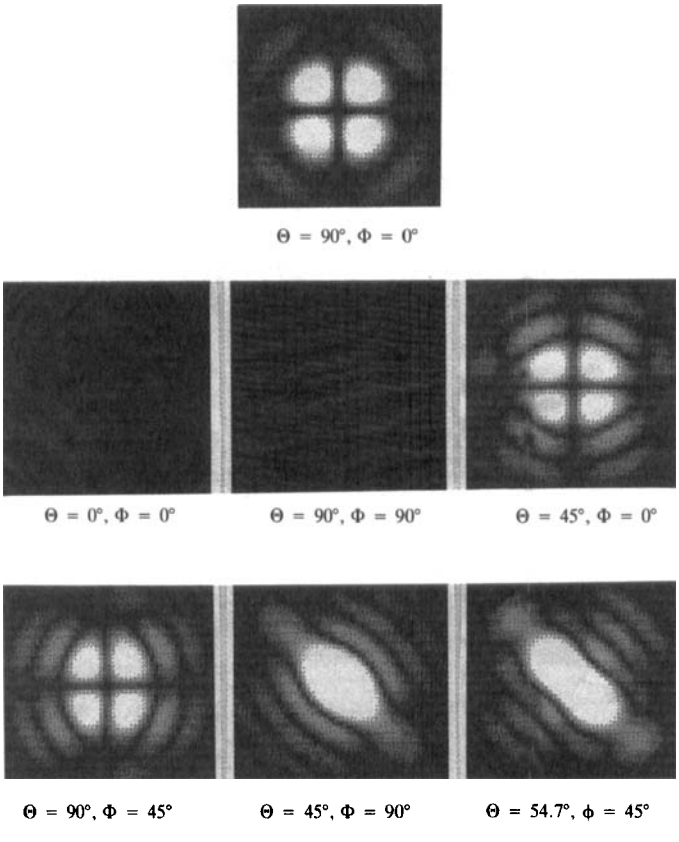


FIGURE 3 Calculated $H_v$ scattering patterns for seven typical orientations of the axial nematic droplet. The orientational angles of the droplet axis, $\Theta$ and $\Phi$, are noted below each corresponding scattering pattern. ($\lambda_m$ = 0.6328 μm; $R$ = 10 μm; area shown: 8° × 8° for $\vartheta$).

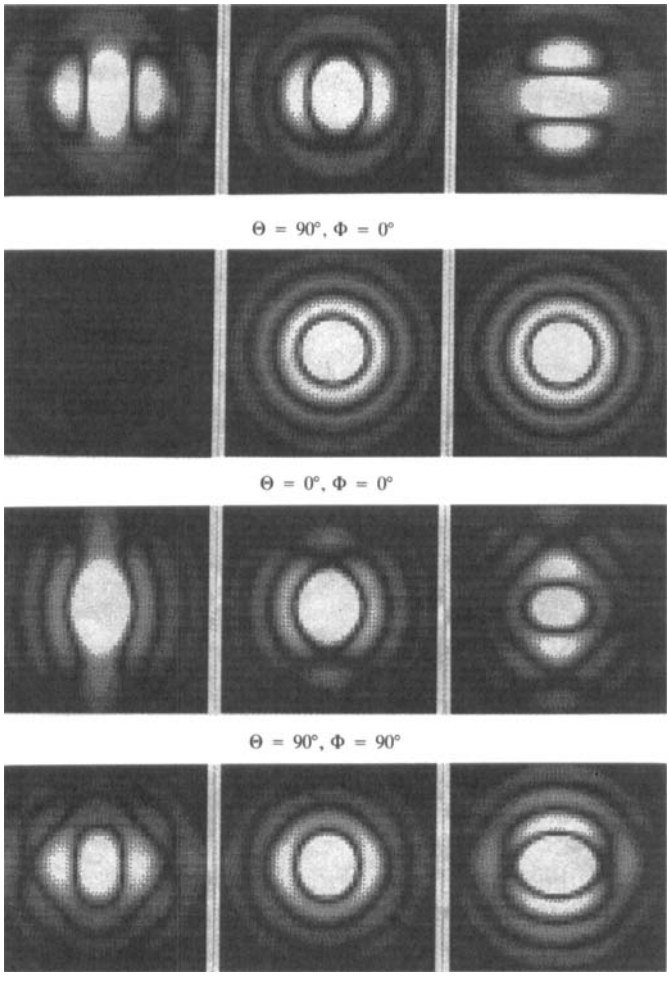


FIGURE 4 Calculated $V_v$ scattering patterns for seven typical orientations of the axial nematic droplet under three groups of relative polarizabilities, ($\alpha_{12}$, $\alpha_{20}$). Other parameters are the same as those in Figure 3 (Continued on next page).

orientation of the droplet axis. The scattering pattern with ($\alpha_{12}$, $\alpha_{20}$) taking the proportion of (1, 0), may be regarded as a key to describing a series of $V_v$ scattering patterns with different relative polarizabilities. This suggests that the relative polarizabilities of many anisotropic systems such as PDLC films can be estimated by $V_v$ light scattering.

### 3.2. Scattering Patterns for the Random Orientation of Axial Nematic Droplets

Droplet axes will be oriented randomly if no external field is imposed on the PDLC film in the sample preparation. We may assume that the scattering from different droplets is incoherent because the positions of nematic droplets are usually dis-

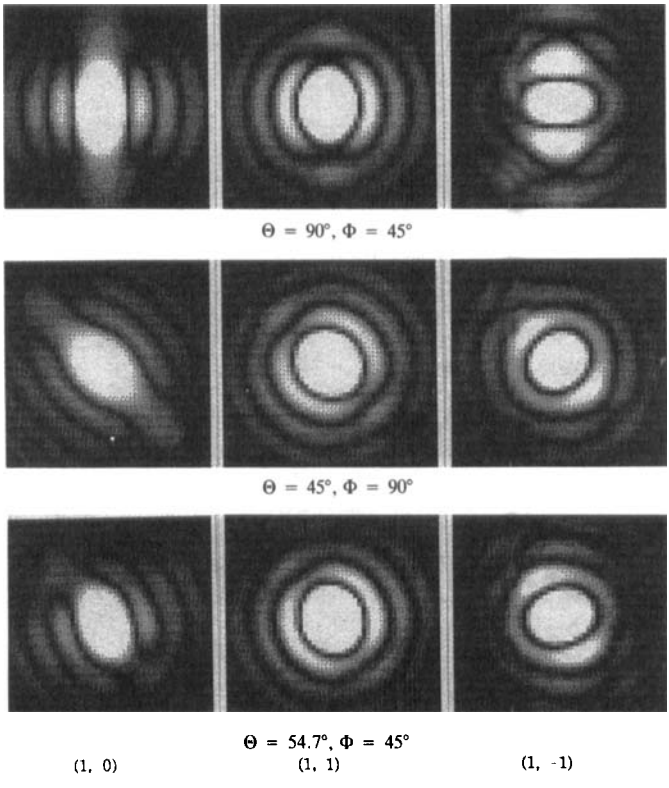


FIGURE 4 (*Continued*)

tributed randomly, thus the total scattered intensity is the sum of the scattered intensities by all nematic droplets with various orientations of droplet axis.

$$I = \int_0^{2\pi} \int_0^{\pi} I(\Theta, \Phi)\sin\Theta \, d\Theta \, d\Phi \Big/ \int_0^{2\pi} \int_0^{\pi} \sin\Theta \, d\Theta \, d\Phi \tag{34}$$

In our calculation, the integration is converted into the following summation:

$$I = \sum_{j=1}^{180/\Delta\Theta} \sum_{k=1}^{180/\Delta\Phi} I(\Theta_j, \Phi_k)\sin\Theta_j \Delta\Theta\Delta\Phi \Big/ \left[ 180 \sum_{j=1}^{180/\Delta\Theta} \sin\Theta_j \Delta\Theta \right] \tag{35}$$

Calculated results indicate that it is fine enough to take $\Delta\Theta = 10°$ and $\Delta\Phi = 18°$. Corresponding $H_v$ and $V_v$ scattering patterns are shown in Figures 5 and 6, respectively. For comparison, the $V_v$ scattering from an isotropic sphere is also presented in the first pattern of Figure 6.

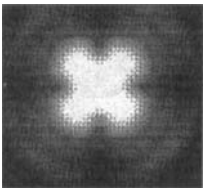

FIGURE 5 Calculated $H_s$ scattering pattern for the random orientation of axial nematic droplets. The parameters are the same as those in Figure 3.

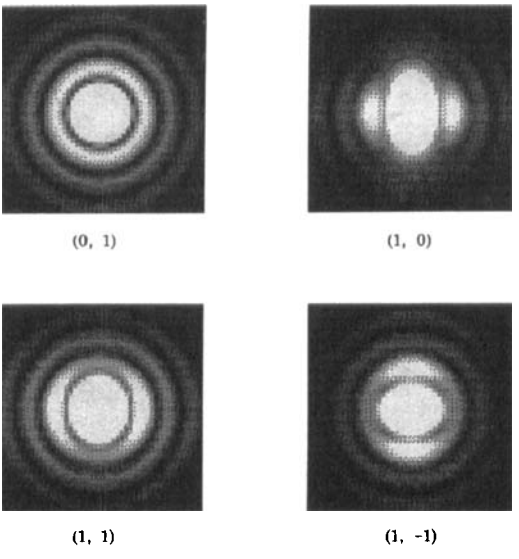


FIGURE 6 Calculated $V_s$ scattering patterns for the random orientation of axial nematic droplets under four groups of relative polarizabilities, ($\alpha_{12}$, $\alpha_{20}$). Here, the case of (0, 1) represents the $V_s$ scattering from an isotropic sphere actually. Other parameters are the same as those in Figure 3.

## 4. RESULTS AND DISCUSSIONS

The expressions for the scattered amplitudes from a radial droplet or a polymer spherulite[4,5] are rewritten first in order to compare SALS from the axial nematic droplet with that from a radial one:

$$E_{H_s} = KE_0V\frac{3}{U^3}\alpha_{12}\cos^2\frac{\vartheta}{2}\sin\mu\cos\mu(4\sin U - U\cos U - 3SiU) \quad (36)$$

$$E_{V_s} = KE_0V\frac{3}{U^3}\left\{\alpha_{20}(\sin U - U\cos U) + \alpha_{12}\left[SiU - \sin U + \cos^2\frac{\vartheta}{2}\cos^2\mu(4\sin U - U\cos U - 3SiU)\right]\right\} \quad (37)$$

where

$$SiU = \int_0^u \frac{\sin x}{x}\, dx \tag{38}$$

Corresponding $H_v$ and $V_v$ scattering patterns are shown in Figures 7 and 8.

According to this paper, director configurations of nematic droplets can be distinguished and the average droplet size can be measured by SALS.

### 4.1. Characterization of Director Configurations

The $H_v$ scattering pattern for a single radial droplet has four disconnected main leaves and the $V_v$ scattering pattern with the anisotropic type has two leaves oriented along $\mu = 90°$, while the scattering patterns for seven typical orientations of the axial nematic droplets have their own characteristics. The leaf-orientations in the $V_v$ scattering patterns for the axial nematic droplet are along the contrary direction

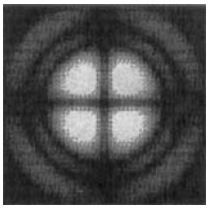

FIGURE 7 Calculated $H_v$ scattering pattern for a radial nematic droplet. The parameters are the same as those in Figure 3.

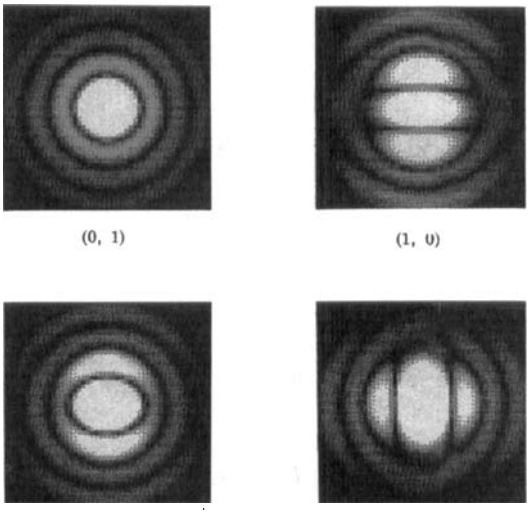


FIGURE 8 Calculated $V_v$ scattering patterns from a radial nematic droplet under four groups of relative polarizabilities, ($\alpha_{12}$, $\alpha_{20}$). Other parameters are the same as those in Figure 3.

with that for a radial one with the same relative polarizabilities. The reason lies in the fact that the axial directors are aligned tangentially instead of radially. The calculated results show that the difference between the $H_v$ or $V_v$ scattering patterns given above is large enough to distinguish the axial and radial director configurations, and further to determine the orientations of the axial nematic droplet.

As for the axial nematic droplets with the random orientation of droplet axes, the leaves of $V_v$ scattering patterns with the anisotropic type are oriented along $\mu = 0°$. All of the $V_v$ scattering patterns have circle or quasicircle outlines. The $H_v$ scattering pattern in this case looks like connected four leaves with two obvious characteristics: no light extinction appears along $\mu = 0°$ and $\mu = 90°$, and the position of the maximum scattered intensity is located at the center. Therefore, even the axial nematic droplets with the random orientation of droplet axes can be discriminated by SALS from the radial droplets and from the axial droplets but with different orientations.

### 4.2. Measurement of Droplet Sizes

The determination of the angular position $\vartheta_m$ of the $H_v$ scattering maximum affords a rapid means for measuring the average size of droplets by use of the relation between $\vartheta_m$ and $R$. For the radial nematic droplet, the formula is: $U = (4\pi R/\lambda_m)\sin(\theta_m/2) = 4.09$, which is very useful in studies on polymer spherulites.[4]

There are no $H_v$ scatterings from the axial nematic droplets with $(\Theta, \Phi)$ taking $(0°, 0°)$ and $(90°, 0°)$. But the scatterings from the axial nematic droplets with $(\Theta, \Phi)$ taking $(90°, 0°)$ and with the random orientation of droplet axes can be observed and these two cases might occur most probably. Since the scattering maximum for the latter is located at the center of the $H_v$ scattering pattern, only the positions of the sub-maximum scattering, namely, the positions of the maximum intensities in four small leaves at relatively large $\vartheta$ in Figure 5, can be detected. In principle, these small leaves can also be used to determine the average size of scattered entities.

Similar to the case of the polymer spherulites or the radial nematic droplets, the azimuthal angles at the scattering maxima in these two cases about the axial nematic droplets are always along $\mu = \pm 45°$ with the average droplet size changed, whereas corresponding scattering angles are never fixed. A series of $\vartheta_m$ under different radii of the axial nematic droplets are calculated, from which the formulae to measure the average sizes are obtained: $U = 4.31$ at the position of the scattering maximum for the axial nematic droplets with $(\Theta, \Phi)$ taking $(90°, 0°)$; $U = 5.56$ at the position of the sub-maximum scattering for the axial nematic droplets with the random orientation of droplet axes.

## 5. CONCLUSIONS

From this study, we conclude that SALS can serve to distinguish the axial nematic droplets from radial ones, and to discriminate the orientations of the droplet axes for the axial nematic droplets. Furthermore, it can serve to estimate the relative polarizabilities of PDLC films by $V_v$ scattering, last but not least, to measure the

average size of nematic droplets by $H_v$ scattering. It should be noted that these results would also be suitable completely for crystalline objects, provided that they had the same director configurations as the axial and radial liquid crystalline droplets. The method used in this paper can be extended to deal with more complex nematic droplets such as the bipolar droplets. Smectic and cholesteric liquid crystals may also be investigated by SALS. The authors would like to promise that SALS will be a very powerful technique to study anisotropic systems with various self-organized structures.



## Acknowledgment

The authors gratefully acknowledge the financial supports from NSF of China and FEYUT of SEDC.

## References

1. M. Kerker. *The Scattering of Light and Other Electromagnetic Radiation* (Academic, New York, 1969).
2. H. C. van de Hulst, *Light Scattering by Small Particles* (Wiley, New York, 1957).
3. C. F. Bohren and D. R. Hoffman, *Absorption and Scattering of Light by Small Particles* (Wiley, New York, 1983).
4. R. S. Stein and M. B. Rhodes, *J. Appl. Phys.*, **31**, 1873 (1960).
5. R. J. Samules, *J. Polym. Sci. A*, **2**, 2163 (1971).
6. R. J. Samules, *Structured Polymer Properties* (John Wiley and Sons, Inc., New York, 1974).
7. P. S. Drzaic, *Mol. Cryst. Liq. Cryst.*, **154**, 289 (1988).
8. J. L. Fergason, *SID (Society for Information Display) Ins. Symp. Dig. Tech. Papers*, **16**, 68 (1985).
9. P. S. Drzaic, *J. Appl. Phys.*, **60**, 2142 (1986).
10. J. W. Doane, N. A. Vaz, B. G. Wu and S. Zumer, *Appl. Phys. Lett.*, **48**, 269 (1986).
11. J. L. West. *Mol. Cryst. Liq. Cryst.*, **157**, 427 (1988).
12. J. Ding and Y. Yang, *Jpn. J. Appl. Phys.*, **31**, 2837 (1992).
13. P. G. de Gennes, *The Physics of Liquid Crystals* (Clarendon, Oxford, 1974).
14. J. H. Erdman, S. Zumer and J. W. Doane, *Phys. Rev. Lett.*, **64**, 1907 (1990).
15. A. Golemme, S. Zumer, J. W. Doane and M. E. Neubert, *Phys. Rev. A*, **37**, 559 (1988).
16. S. Zumer and J. W. Doane, *Phys. Rev. A*, **34**, 3373 (1986).
17. S. Zumer, *Phys. Rev. A*, **37**, 4006 (1986).
18. R. D. Sherman, *Phys. Rev. A*, **40**, 1591 (1989).
19. S. Zumer, A. Golemme and J. W. Doane, *J. Opt. Soc. Am. A*, **6**, 403 (1989).
20. J. Ding and Y. Yang, accepted by *J. Phys. D.*